Title

Extremophile-based biohybrid micromotors for biomedical operations in harsh acidic environments

Journal

Science Advances, 8(51)

ISSN

2375-2548

Authors

Zhang, Fangyu
Li, Zhengxing
Duan, Yaou
et al.

Publication Date

2022-12-23

DOI

10.1126/sciadv.ade6455

Peer reviewed

ENGINEERING

Extremophile-based biohybrid micromotors for biomedical operations in harsh acidic environments

Fangyu Zhang†, Zhengxing Li†, Yaou Duan†, Hao Luan, Lu Yin, Zhongyuan Guo, Chuanrui Chen, Mingyao Xu, Weiwei Gao, Ronnie H. Fang, Liangfang Zhang*, Joseph Wang*

The function of robots in extreme environments is regarded as one of the major challenges facing robotics. Here, we demonstrate that acidophilic microalgae biomotors can maintain their swimming behavior over long periods of time in the harsh acidic environment of the stomach, thus enabling them to be applied for gastrointestinal (GI) delivery applications. The biomotors can also be functionalized with a wide range of cargos, ranging from small molecules to nanoparticles, without compromising their ability to self-propel under extreme conditions. Successful GI delivery of model payloads after oral administration of the acidophilic algae motors is confirmed using a murine model. By tuning the surface properties of cargos, it is possible to modulate their precise GI localization. Overall, our findings indicate that multifunctional acidophilic algae-based biomotors offer distinct advantages compared to traditional biohybrid platforms and hold great potential for GI-related biomedical applications.

INTRODUCTION

The operation and navigation of robots in extreme environments have been listed as one of the 10 grand challenges facing robotics in the next decade (*1*). Recent robotic research along these lines has focused primarily on developing macroscale robots for operation in challenging environments, such as deep oceans with high pressure (*2*), polar regions with low temperature (*3*), and deserts with high temperature (*4*). Upon scaling to the microscale regime, robots face additional challenges associated with propulsion in a low Reynolds number medium. Over the past decade, various microrobotic platforms have been developed to meet the propulsion requirements for diverse biomedical and environmental applications using three motion mechanisms, including energy harvesting from external fields (*5*–*9*), reaction with fuels present in the local surroundings (*10*–*15*), or using the intrinsic motility and natural taxis behavior of living biological organisms (*16*–*20*). Microrobotic platforms can provide distinctive advantages for in vivo operations by leveraging their active propulsion to deliver therapeutics to specific sites within the body (*21*–*26*). Notably, micromotors have recently emerged as powerful tools for effective oral drug delivery, helping to address several limitations of traditional oral drug formulations such as poor drug absorption, short retention, and low bioavailability (*27*, *28*). However, the extended operation of micromotors in the highly acidic gastric environment is still challenging and requires the development of innovative solutions (*29*).

Although several studies have aimed at integrating self-actuating mechanical devices in millimeter-sized robotic pills for application in the harsh conditions of the gastrointestinal (GI) tract (*30*–*32*), effective and long-term operation of micromotors in an extremely acidic medium (pH < 3) remains highly challenging owing to its ability to corrode or degrade various types of micromotor platforms. There are only few reports on the influence of extremely acidic conditions on the movement of micromotors. For example, coating magnetically powered microswimmers with Al_2O_3 films was reported to enhance their propulsion in acidic conditions (*33*). Al/Pd spherical micromotors were shown to operate in a wide range of pH conditions (*34*). Last, the self-propulsion of zinc microrockets and magnesium-based Janus micromotors in the gastric environment has led to enhanced therapeutic GI delivery (*35*, *36*). Although synthetic micromotors have demonstrated utility for GI applications, their short lifetimes in acidic conditions limit their practical use to only short segments within the GI tract. Prolonged operation in the gastric and intestinal fluid can endow micromotors with the ability to actively drive therapeutic payloads to widely distributed areas over the entire GI tract and enhance the dispersion and retention of drugs for treating diseases and disorders. It is clear that realizing efficient and prolonged micromotor operation in a highly acidic medium remains an important unmet need, particularly for biomedical applications in the gastric environment.

In this work, we demonstrate an extremophile-based biohybrid micromotor capable of continuous and prolonged operation in extremely low pH environments. Many extremophiles, capable of surviving under extreme physical or chemical conditions, are found in some of the harshest environments on earth (*37*). Among them, acidophilic microalgae have been shown to support the ecosystems of extremely acidic environments scattered around the globe associated with sulfur springs, volcanic vents, and acid mine drainages (*38*). These acidophilic algae evolved from their respective neutrophilic ancestors to thrive at low pH by reducing their proton influx and increasing their proton pump efficiency (*39*, *40*). Here, we demonstrated the efficient and prolonged motion behavior of acidophilic algae in strong hydrochloric acid down to pH 1 and their tremendous potential for microrobotic GI delivery applications. Specifically, we relied on *Chlamydomonas pitschmannii*, an acidophilic alga isolated from an acid mine drainage (*41*). *C. pitschmannii* displayed a negligible change in speed over an extremely broad pH range, from pH 1 to 10, compared to the neutrophilic alga *Chlamydomonas reinhardtii*, which was incapable of swimming in acidic

Department of NanoEngineering and Chemical Engineering Program, University of California San Diego, La Jolla, CA 92093, USA.
*Corresponding author. Email: josephwang@ucsd.edu (J.W.); zhang@ucsd.edu (L. Z.)
†These authors contributed equally to this work.

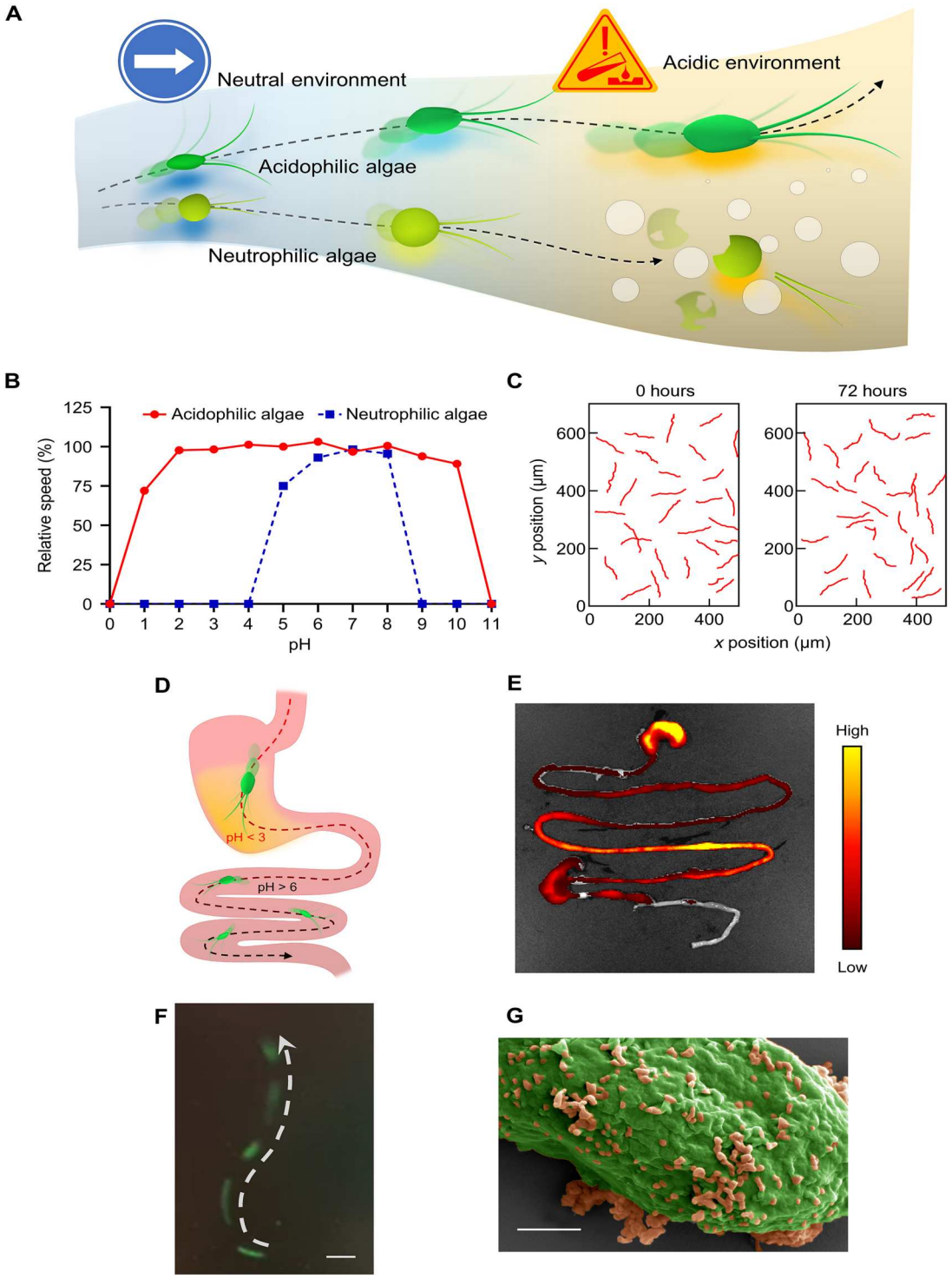

Fig. 1. Schematics of acidophilic algae micromotors for various biomedical applications. (**A**) Acidophilic algae motors are capable of prolonged motion in both neutral and acidic environments, whereas neutrophilic algae are incapable of operating in highly acidic environments. (**B**) The relative speed of acidophilic algae and neutrophilic algae over a range of pH values compared to their speed in optimal culture conditions (modified acidic medium at pH 3.5 for acidophilic algae; tris-acetate-phosphate at pH 7 for neutrophilic algae). (**C**) Two-dimensional motion trajectories of acidophilic algae motors over a period of 1 s before and 72 hours after swimming in HCl at pH 1.5. (**D**) Acidophilic algae motors can operate throughout the entire GI tract for in vivo delivery applications. (**E**) Representative biodistribution of acidophilic algae motors in the GI tract at 2 hours after administration by oral gavage. (**F**) One-second motion trajectory of acidophilic algae-based biohybrid motors carrying dye-labeled nanoparticles in HCl at pH ~ 1.5. Scale bar, 10 μm. (**G**) Representative pseudo-colored scanning electron microscopy (SEM) image of a nanoparticle-functionalized acidophilic algae motor. Scale bar, 1 μm.

medium (pH < 4) and rapidly degraded (Fig. 1, A and B). Notably, the movement of *C. pitschmannii* in the acidic medium was maintained over an extended period of at least 72 hours (Fig. 1C, fig. S1, and movie S1). We further evaluated the performance of the acidophilic biomotors in gastric fluid (pH 1.5) and intestinal fluid (pH 6.5) and tracked their in vivo biodistribution to establish their potential for biomedical applications involving GI tract delivery (Fig. 1, D and E). Multifunctional biohybrid algae motors were fabricated by decorating the acidophilic algae with polymeric nanoparticles, which were loaded with a green fluorescent dye for visualization purposes (Fig. 1F). The binding between nanoparticles and *C. pitschmannii* algae was clearly observed by electron microscopy (Fig. 1G). Last, by tuning the surface properties of the cargo, selective targeting to the stomach or broad GI tract delivery could be achieved. The effective and long-term movement of cargo-loaded acidophilic algae motors over a wide range of pH conditions, including harsh acidic media, along with their strong retention in the GI tract, suggests that the platform holds considerable promise for future biomedical applications in the GI tract. Further work on extremophile-based multifunctional biohybrid micromotors could lead to the development of microrobotic platforms capable of excelling in a variety of harsh environments.

RESULTS

Motion behavior of acidophilic algae

C. pitschmannii CPCC 354 was selected as a model acidophilic algae strain, and its swimming behavior was characterized in extremely acidic conditions. To evaluate their movement, the algae were cultured in a modified acidic medium (MAM) (*42*) (pH 3.5) to a density of 1×10^6/ml, followed by transfer to hydrochloric acid for speed measurement. The algae exhibited constant swimming with a speed of 95 to 105 μm/s (corresponding to ~10 body length/s) in an extremely acidic environment at pH 1.5 (Fig. 2A, fig. S2, and movie S2). Their movement was also tracked over a 5-s period under the same condition to visualize a representative trajectory (Fig. 2B and movie S3). When investigating the tolerance range of the algae to extreme acid, we found that they displayed a notable decrease in speed and loss of activity after 1 hour of motion at pH 1 (Fig. 2C, fig. S3, and movie S4). Furthermore, the effect of the anion was evaluated by immersing the algae in different common strong acids (HCl, H_2SO_4, and HNO_3) adjusted to pH 1.5 (Fig. 2D, fig. S4, and movie S5). The detrimental effect of nitric acid on the algae motion could be explained by its strong oxidizing capacity compared to the other two acids.

We observed that the acidophilic algae could not only resist extreme acidic conditions (pH < 3) but also able to survive in neutral and alkaline environments (Fig. 2E and fig. S5). After 30 min of adaptation, the acidophilic algae displayed efficient movement across a broad pH range from 1 to 10 (Fig. 2F, fig. S6, and movie S6). In comparison, a model neutrophilic algae *C. reinhardtii*, which have been commonly used as microorganism-based micromotors for various environmental and biomedical applications (*17*, *20*, *26*, *43*), were unable to tolerate extreme acidic pH and could swim only over a narrow pH range between 5 and 8 (Fig. 2F, fig. S7, and movie S7). The contrast between the two types of algae was further highlighted by visualizing their trajectories at pH 1.5, 4, and 7 after various periods of time (Fig. 2, G and H, and movies S8 and S9). Only slight speed differences were observed for the acidophilic algae at all pH values after 24 hours, whereas the motility of neutrophilic algae rapidly diminished at pH 1.5 and 4.

Biodistribution and retention of acidophilic algae in the GI tract

The oral route of administration is the most common approach for drug delivery to treat GI disease (*44*). A major challenge of GI delivery is overcoming the physiological barrier caused by the extreme acidity within the stomach. To investigate the potential of acidophilic algae biomotors for improved GI delivery, we first tested their motion ability and viability in vitro in simulated gastric (pH ~ 1.5) and intestinal (pH ~ 6.5) fluids (fig. S8). They exhibited good adaptation in both physiological fluids, and their self-propulsion (~100 μm/s) was unaffected after 8 hours of constant movement, indicating great promise for in vivo GI operation. In comparison, the neutrophilic algae lost their motion ability rapidly upon transfer from the culture medium to gastric fluid at room temperature (fig. S9, A and B). We also observed for any changes in morphology using electron microscopy after incubation in strong gastric acid. The acidophilic algae displayed an intact structure after 2 hours of motion, whereas the neutrophilic algae were structurally damaged after the same period of time (fig. S9, C and D). To further mimic the physiological conditions in the stomach (*45*), we assessed the speed and lifetime of acidophilic algae in simulated gastric fluid containing pepsin (1 mg/ml) at body temperature (37°C) and found that the algae maintained speeds of 65 and 35 μm/s after 1 and 2 hours of incubation, respectively (fig. S10). These results supported the potential of the acidophilic algae for active transport throughout the GI tract, whereas the regular neutrophilic algae would be unable to traverse the harsh acidic medium in the stomach.

Next, we demonstrated the distinct advantages of acidophilic algae biomotors for GI delivery by examining their biodistribution and retention after oral administration using a murine model. Ex vivo fluorescence imaging was conducted to determine the influence of acid tolerance on algae localization within the GI tract (Fig. 3, A to C). To visualize and track the algae, their surfaces were covalently bound with the near-infrared fluorescent dye Cyanine7 (Cy7) ($\lambda_{ex}/\lambda_{em}$ = 750 nm/773 nm) (*46*), which did not hinder their motion behavior in GI fluid (fig. S11). Before oral gavage, we confirmed that the dye-conjugated acidophilic algae, neutrophilic algae, and alkaline-treated static acidophilic algae were similar in number and fluorescence intensity (fig. S12). At various time points (0.5, 2, 5, 10, and 24 hours) after oral administration, the mice were euthanized, and their GI tracts were isolated to visualize the location of algae. As shown in Fig. 3A, the acidophilic algae displayed a strong signal throughout the entire GI tract, showing sustained retention in the stomach and wide distribution in the lower GI tract within the first 5 hours. In comparison, the signals from the neutrophilic algae (Fig. 3B) and the static acidophilic algae (Fig. 3C) diminished rapidly within 2 hours after administration. These results emphasized the importance of the acid tolerance and self-propulsion properties of acidophilic algae, which enabled efficient operation in the stomach and effective distribution in the lower GI tract. The visual observations were further corroborated by quantifying the total radiant efficiency in the stomach (Fig. 3D) or in the small intestine and colon (Fig. 3E) at different time points.

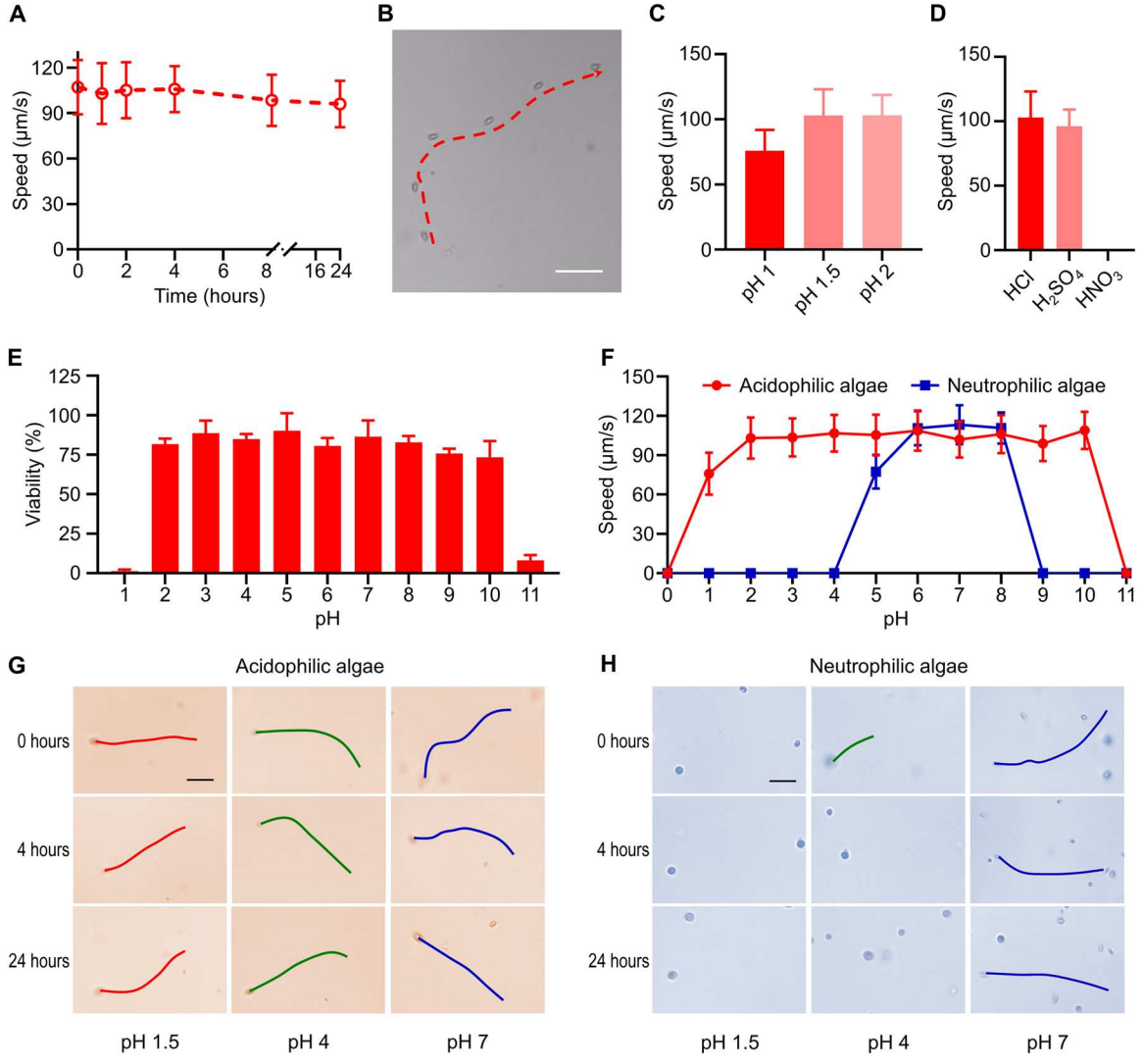

Fig. 2. Motion behavior of acidophilic algae biomotors in extremely acidic conditions. (**A**) Speed of acidophilic algae biomotors at different time points (0, 1, 2, 4, 8, and 24 hours) in HCl at pH 1.5. (**B**) The representative trajectory of an acidophilic alga biomotor over a period of 5 s in HCl at pH 1.5. Scale bar, 100 μm. (**C**) Swimming speed of algae biomotors upon 1 hour of exposure to HCl at pH 1, 1.5, and 2 (n = 100; means + SD). (**D**) Swimming speed of acidophilic algae biomotors in different acidic mediums (HCl, H_2SO_4, and HNO_3) at pH 1.5 (n = 100; means + SD). (**E**) Viability of acidophilic algae in different media at pH values from 1 to 11 (n = 3; means + SD). (**F**) Speed comparison of acidophilic algae with neutrophilic algae at pH between 0 and 11 (n = 100; means ± SD). Speed was measured from 100 individual algae. (**G** and **H**) Representative trajectories over a period of 2 s for acidophilic algae (G) and neutrophilic algae (H) after various durations (0, 4, and 24 hours) of exposure to HCl at pH 1.5, 4, and 7. Scale bars, 50 μm.

Biosafety of acidophilic algae in GI

To assess the safety of the acidophilic algae, we evaluated their toxicity profile both systemically and locally in the lower GI tract. A treatment dosage of 1×10^7 acidophilic algae was orally administered to mice, while untreated mice served as controls. A comprehensive blood chemistry panel and blood cell count were conducted 24 hours afterward (Fig. 4, A and B). There was no statistical difference between the untreated control and the algae treatment group in any of the 14 blood parameters and blood cell populations that were analyzed. Hematoxylin and eosin (H&E)–stained histological sections showed that the stomach and intestinal mucosa or submucosa maintained their integrity without any lymphocyte infiltration or signs of inflammation (Fig. 4C). Last, histological analysis of the major organs, including the heart, liver, spleen, lungs, and kidneys, was performed (Fig. 4D). The appearance of all the organs was normal compared to healthy mice. Further studies will be required to comprehensively evaluate the impact of algae administration on other immune parameters, both local and systemic, across multiple time scales.

Stomach delivery with acidophilic algae motors

Upon confirming the biodistribution and safety of acidophilic algae for GI administration, we evaluated the feasibility of leveraging them for cargo delivery. Poly(lactic-*co*-glycolic acid) (PLGA) nanoparticles were chosen as the model payload because they are attractive for therapeutic delivery applications with properties such as

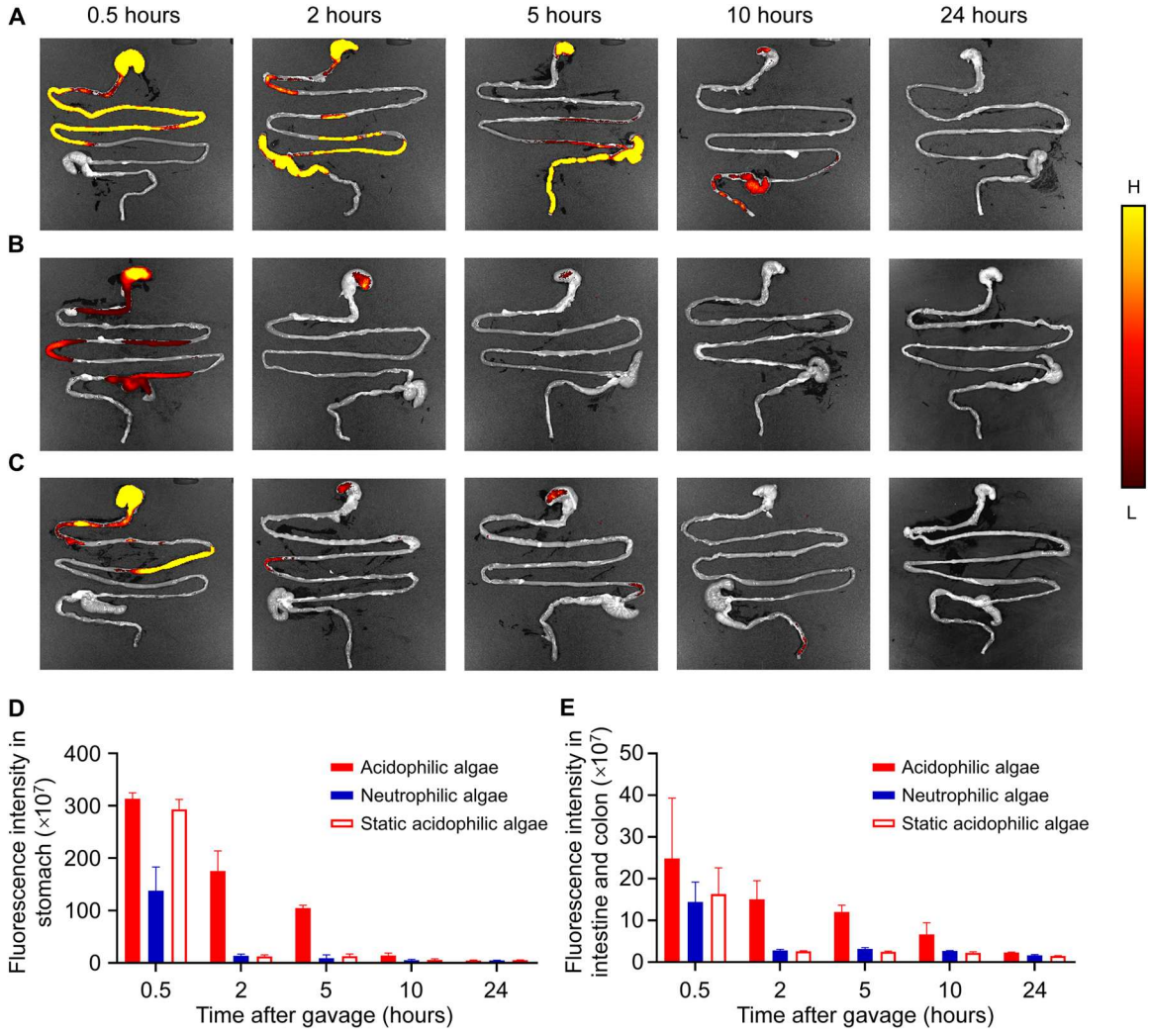

Fig. 3. Biodistribution of acidophilic algae biomotors in the GI tract. (**A** to **C**) Mice were orally gavaged with Cy7-labeled acidophilic algae (A), Cy7-labeled neutrophilic algae (B), or Cy7-labeled static acidophilic algae (C), and distribution in the GI tract was visualized over time. (**D** and **E**) Measurement of the fluorescence intensity in the stomach (D) or small intestine and colon (E) at different time points (0.5, 2, 5, 10, and 24 hours) after oral gavage (n = 3; means + SD).

controlled and sustained drug release, high drug loading yield, and low toxicity (*47*). To fabricate the acidophilic algae biohybrid motors, positively charged poly-L-lysine (PLL)–coated PLGA nanoparticles (denoted as "PLLNP") were attached to the negatively charged acidophilic algae surface via electrostatic interaction, thus generating PLLNP-loaded acidophilic algae biohybrid motors (denoted as "acido-algae-PLLNP") (Fig. 5A). The surface coating on the PLGA core was first optimized by tuning the incubation time between the nanoparticles and the PLL polyelectrolyte to yield PLLNP with a strong positive surface charge (fig. S13). The determination of zeta potential at different pH values is important for complexing two materials based on electrostatic interactions (*48*). To this end, the surface charge of bare acidophilic algae and PLLNP was evaluated at pH values ranging from 1 to 11 (fig. S14). It was found that the PLL coating could promote the effective binding of PLGA nanoparticles to algae at neutral pH, which was visualized by fluorescence microscopy (Fig. 5B). The algae were uniformly surrounded by 3,3′-dioctadecyloxacarbocyanine perchlorate (DiO; $\lambda_{ex}/\lambda_{em}$ = 484/501 nm)–loaded PLLNP. A pseudo-colored scanning electron microscopy (SEM) image illustrated the attachment of the nanoparticles onto the algae cell surface (Fig. 5C). The motion behavior of the acido-algae-PLLNP was characterized by measuring their speed under extreme acidic conditions at pH 1.5 (Fig. 5D). The decreased speed of the acido-algae-PLLNP (~50 μm/s) compared to bare acidophilic algae (~100 μm/s) could be attributed to the influence of the positively charged cargo on the flagella, as indicated by inconsistent (zigzag trajectory) movement patterns (Fig. 5E and movie S10).

Next, we evaluated the gastric cargo delivery ability of the acido-algae-PLLNP biohybrid motors. A near-infrared dye, 1,1′-dioctadecyl-3,3,3′,3′-tetramethylindotricarbocyanine iodide (DiR; $\lambda_{ex}/\lambda_{em}$ = 748/780 nm), was encapsulated into PLLNP as a model payload. Before the animal studies, an in vitro study was conducted to assess the stability of cargo loading on the biohybrid motors (fig. S15). In the acido-algae-PLLNP formulation, released dye or unbound nanoparticles were hardly detected even after 24 hours

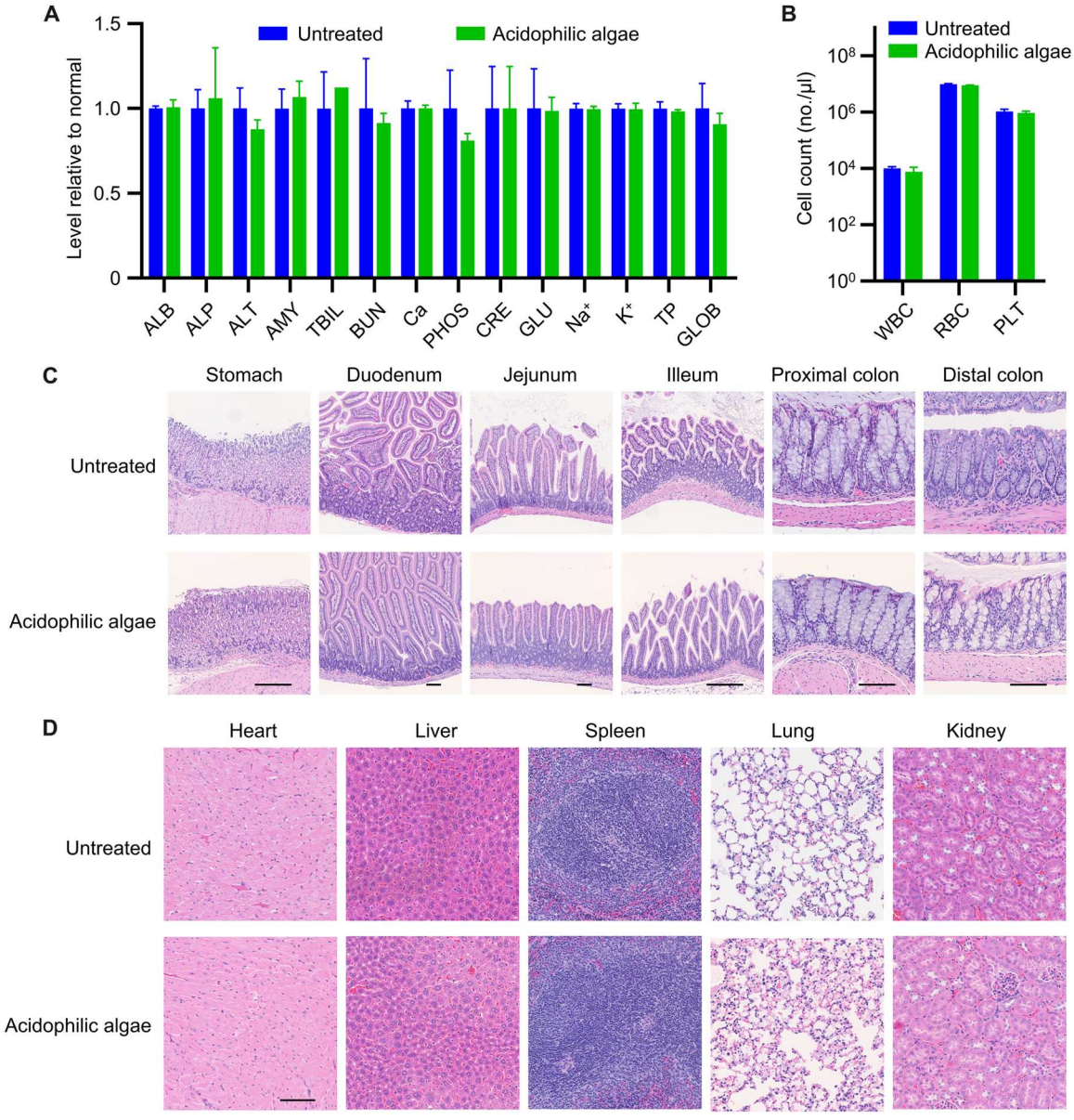

Fig. 4. In vivo safety evaluation of acidophilic algae. (**A**) Comprehensive blood chemistry panel for untreated mice or mice at 24 hours after treatment with acidophilic algae micromotors (n = 3; means + SD). ALB, albumin; ALP, alkaline phosphatase; ALT, alanine transaminase; AMY, amylase; TBIL, total bilirubin; BUN, blood urea nitrogen; Ca, calcium; PHOS, phosphorus; CRE, creatinine; GLU, glucose; Na^+, sodium; K^+, potassium; TP, total protein; GLOB, globulin (calculated). (**B**) Counts for various blood cells taken from untreated mice or mice at 24 hours after treatment with acidophilic algae micromotors (n = 3; means + SD). WBC, white blood cells; RBC, red blood cells; PLT, platelets. (**C**) Representative H&E-stained histology sections of different portions of the GI tract from untreated mice or mice 24 hours after treatment with acidophilic algae micromotors. Scale bars, 100 μm. (**D**) Representative H&E-stained histology sections of major organs from untreated mice or mice at 24 hours after treatment with acidophilic algae micromotors. Scale bar, 100 μm.

of incubation in HCl (pH 2) or simulated gastric fluid (pH 1.5), indicating highly stable cargo binding to the algae via electrostatic interactions, hydrogen bonding between PLL and the diverse functional groups present on the algae surface, and physical entrapment of nanoparticles by the highly porous structure of the algae cell wall. Then, acido-algae-PLLNP and PLLNP control (without algae) were orally administered to mice to study their biodistribution and retention. After 2, 5, and 10 hours, the mice were euthanized, and their GI tracts were isolated for ex vivo imaging (Fig. 5F). Both acido-algae-PLLNP and PLLNP were mainly located in the stomach, which is attributed to the mucoadhesive property of the positively charged PLLNP (*44*). However, the motion of the biohybrid motors enabled a higher chance of contact between the nanoparticles and the luminal lining, facilitating efficient cargo retention in the stomach. This accumulation can be used to improve drug delivery and enhance tissue penetration, as was demonstrated previously using micromotors for oral vaccine delivery (*49*). Quantification of the fluorescence intensity within the stomach

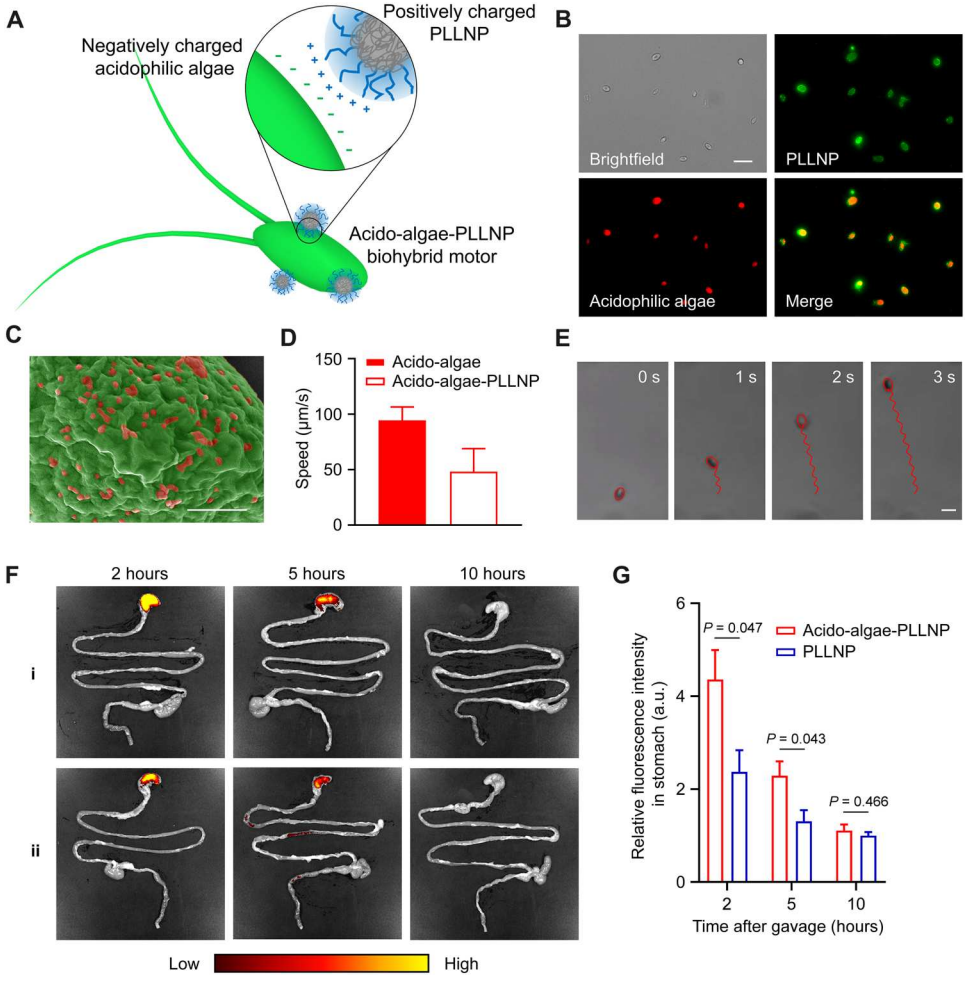

Fig. 5. Acido-algae-PLLNP biohybrid motors for stomach delivery. (**A**) Loading of PLLNP onto acidophilic algae motors by electrostatic interaction. (**B**) Fluorescence microscopy images of acido-algae-PLLNP biohybrid motors. Red, acidophilic algae (chloroplast autofluorescence); green, PLLNP (DiO). Scale bar, 20 μm. (**C**) Pseudo-colored SEM images of an acido-algae-PLLNP biohybrid motor. Scale bar, 1 μm. (**D**) Speed comparison of acido-algae-PLLNP and bare acidophilic algae (denoted as "acido-algae" in the figure) at pH 1.5 (n = 20; means + SD). (**E**) Representative trajectories of the acido-algae-PLLNP biohybrid motor over a period of 3 s in HCl at pH 1.5. Scale bar, 10 μm. (**F**) Ex vivo imaging of the GI tract at 2, 5, and 10 hours after oral administration of acido-algae-PLLNP (i) or PLLNP (ii). (**G**) Fluorescence intensity of the DiR dye delivered by acido-algae-PLLNP or PLLNP in the stomach at 2, 5, and 10 hours after oral gavage (n = 3; means + SD). a.u., arbitrary units.

supported the greatly improved retention of PLLNP when delivered by acido-algae-PLLNP biohybrid motors as opposed to in free form within the first 5 hours after oral gavage (Fig. 5G).

Entire GI delivery with acidophilic algae motors

After confirming effective cargo delivery to the stomach using mucoadhesive PLLNP attached to the surface of acidophilic algae motors, we sought to evaluate whether the acidophilic algae could be used to transport cargo throughout the entire GI tract given their effective distribution shown in Fig. 3. Instead of using positively charged PLLNP, we elected to use PLGA cores with a cell membrane coating, which endows versatile surface functionality and biomimetic properties to nanocarriers (*50*). Red blood cell (RBC) membrane–coated PLGA nanoparticles (denoted as "RBCNP") were prepared on the basis of a previously established protocol (*51*). The hydrodynamic size and zeta potential of RBCNP were characterized by dynamic light scattering, indicating the slight increase in size and negative charge after membrane coating (fig. S16, A and B). The RBC membrane coating onto the PLGA surface was further verified by transmission electron microscopy, showing an intact core-shell structure (fig. S16C). To achieve the loading of RBCNP onto algae, a bioorthogonal conjugation approach using copper-free click chemistry was used (Fig. 6A) (*52*). Briefly, the algae and RBCNP were separately functionalized with dibenzocyclooctyne–(-polyethylene glycol)$_4$–*N*-hydroxysuccinimidyl ester (DBCO-PEG$_4$-NHS) and azido-PEG$_4$-NHS ester, respectively. The two components were then conjugated together by leveraging these newly introduced functional groups. The attachment of RBCNP to acidophilic algae (denoted as "acido-algae-RBCNP") was validated by a pseudo-colored SEM image (Fig. 6B) and fluorescent imaging, confirming the effective binding between DiO dye–labeled RBCNP and the algal surface (Fig. 6C). The covalent binding of RBCNP had minimal effects on the motion behavior (speed and tracking pattern) of the algae motors (Fig. 6, D and E). After 24 hours of incubation in acidic fluid, 90% of the fluorescence intensity of DiR-loaded RBCNP onto the algae surface was preserved, indicating the

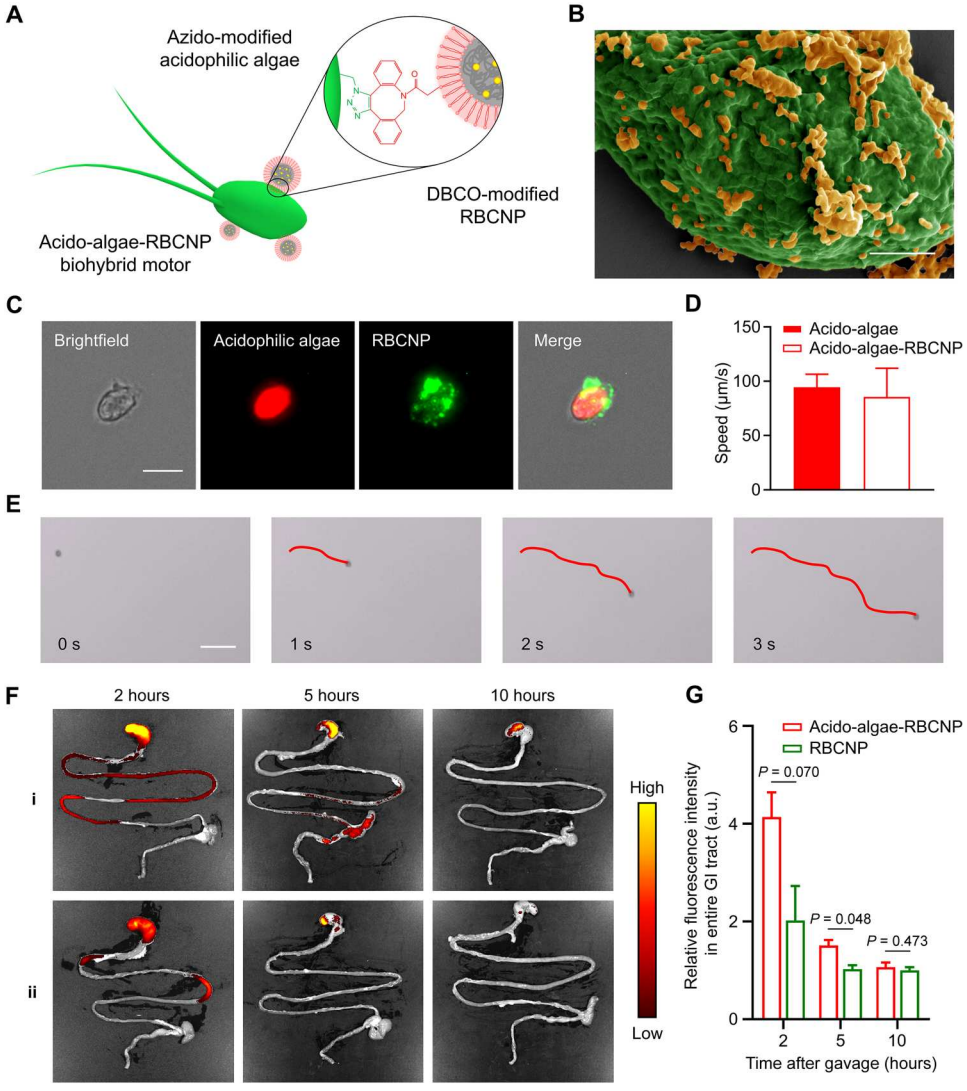

Fig. 6. Acido-algae-RBCNP biohybrid motors for entire GI tract delivery. (**A**) Loading of RBCNP onto acidophilic algae motors via click chemistry. (**B**) Pseudo-colored SEM image of an acido-algae-RBCNP biohybrid motor. Scale bar, 1 μm. (**C**) Representative fluorescence microscopy images of an acido-algae-RBCNP biohybrid motor. Red, acidophilic algae (chloroplast autofluorescence); green, RBCNP (DiO). Scale bar, 10 μm. (**D**) Speed comparison of acido-algae-RBCNP and bare acidophilic algae (denoted as "acido-algae" in the figure) at pH 1.5 (n = 20; means + SD). (**E**) Representative trajectories of acido-algae-RBCNP biohybrid motor over a period of 3 s in HCl at pH 1.5. Scale bar, 50 μm. (**F**) Ex vivo imaging of the GI tract at 2, 5, and 10 hours after oral administration of acido-algae-RBCNP (i) or RBCNP (ii). (**G**) Fluorescence intensity of the DiR dye delivered by acido-algae-RBCNP or RBCNP in the entire GI at 2, 5, and 10 hours after oral gavage (n = 3; means + SD).

high binding stability between acidophilic algae and RBCNP in a harsh acidic environment (fig. S17).

Next, we evaluated the feasibility of using acido-algae-RBCNP biohybrid motors for delivery throughout the GI tract. DiR was loaded into RBCNP as a model payload to track nanoparticle localization at different GI sites in vivo. At 2, 5, and 10 hours after oral administration of acido-algae-RBCNP and free RBCNP (without algae) with a similar amount of DiR loading, the GI tract was excised for ex vivo fluorescence imaging (Fig. 6F). Because of their acid tolerance and movement capabilities, the acido-algae-RBCNP motors were able to transport the RBCNP to the entire GI tract as opposed to only the stomach. The fluorescent signals from the active biohybrid motor group were more substantial in both the stomach and the small intestine at 2 hours and remained stronger at 5 and 10 hours when compared with the free RBCNP group. Note that the 10-hour cargo retention facilitated by the biohybrid motors was much longer than the gastric emptying time of a fluid meal (*53*). A similar trend of improved GI payload retention by acido-algae-RBCNP was confirmed when quantifying the fluorescent signals, with 2-fold and 1.5-fold enhancement at 2 and 5 hours after oral gavage, respectively (Fig. 6G). These results confirmed that controlling the surface properties of the nanoparticle payload could selectively position the biohybrid motors in different regions of the GI tract.

DISCUSSION

In summary, we have reported on the first extremophile-based algae biohybrid motor for application in harsh conditions such as acidic biological fluid. Acidophilic *C. pitschmannii* algae were chosen based on the basis of their ability to effectively swim in highly acidic conditions. The unique adaptability and long-lasting self-propulsion of the acidophilic algae over a wide pH range (1.5 to 10) provided the natural micromotor essential flexibility for efficient performance in both gastric and intestinal fluid. In a murine model, oral administration of the acidophilic algae resulted in improved GI distribution and retention compared to neutrophilic algae and static acidophilic algae controls. By functionalizing the algae with cargo-loaded PLGA nanoparticles via different conjugation approaches, the resulting multifunctional biohybrid micromotors were able to facilitate cargo delivery to the stomach or the entire GI tract in vivo. Once inside the GI tract, the PLGA nanoparticles provide controlled and sustained drug release through the hydrolytic cleavage of their polyester backbones (*54*). While the current surface attachment strategies were effective for loading drug onto the algae motors, other approaches such as the incorporation of small-molecule drugs inside the algae could be explored (*55*). In addition, various drug payloads, including chemotherapeutics and biologics, could be incorporated to improve their therapeutic activity for local GI diseases (*56*). Long-term biosafety monitoring needs to be performed before the clinical studies of the biohybrid motors to verify their lack of immunogenicity and toxicity. Looking forward, we envision the decoration of the acidophilic algae with multiple functional units, including therapeutics, contrast agents, targeting moieties, and magnetic particles to create multifunctional microrobotic platforms with accurate maneuverability for targeted GI drug delivery. Overall, extremophile-based biohybrids offer considerable promise and open the door for diverse applications in harsh and inhospitable environments that are unsuitable for traditional microrobots.

MATERIALS AND METHODS

Algae culture

The acidophilic algae *C. pitschmannii* (strain CPCC-354 wild-type) were obtained from the Canadian Phycological Culture Centre (CPCC). The algae were transferred from their original medium to MAM (CPCC) and cultivated at room temperature under cycles of 12-hour sunlight and 12-hour darkness. The neutrophilic algae *C. reinhardtii* (strain CC-125 wild-type mt+) were obtained from the Chlamydomonas Resource Center. The algae were transferred from the agar plate to tris-acetate-phosphate medium (Thermo Fisher Scientific) and cultured under the same conditions.

Preparation of dye-conjugated acidophilic algae

Acidophilic algae were transferred from the culture medium to 1× phosphate-buffered saline (PBS; Thermo Fisher Scientific) followed by three washes. Next, NHS-Cy7 (10 μg/ml; Lumiprobe) was incubated with the algae at 1×10^7/ml for 1 hour at room temperature. After dye conjugation, the modified algae were washed with ultrapure water for the removal of the unreacted dye and resuspended in ultrapure water for further use. Static acidophilic algae were prepared through the dropwise addition of 1 M acetic acid (Sigma-Aldrich) to active acidophilic algae. After 20 s, the pH value of the mixture was quickly neutralized to 7 by the addition of 1 M sodium hydroxide (Sigma-Aldrich), and the algae were transferred into PBS. Then, the Cy7 dye conjugation was performed following a similar method as above. Neutrophilic algae were suspended in 10 mM Hepes (Thermo Fisher Scientific) to complete the Cy7 conjugation.

Synthesis of fluorescent dye–loaded polymeric nanoparticles

The synthesis of polymeric nanoparticles was based on a previously reported nanoprecipitation method (*51*). Briefly, carboxyl-terminated 50:50 PLGA (0.67 dl/g; LACTEL Absorbable Polymers) at 20 mg/ml in 1 ml of acetone was added into 1 ml of 10 mM tris buffer. To fluorescently label the nanoparticles, 0.1 weight % (wt %) of DiO ($\lambda_{ex}/\lambda_{em}$ = 484 nm/501 nm; Thermo Fisher Scientific) was encapsulated into the PLGA cores. After nanoprecipitation, the organic solvent was evaporated under a vacuum for 1 hour. Near-infrared dye-loaded polymeric nanoparticles for in vivo studies were prepared following a similar method by replacing DiO with DiR ($\lambda_{ex}/\lambda_{em}$ = 748 nm/780 nm; Thermo Fisher Scientific).

Preparation of PLLNP

To prepare the PLGA nanoparticles coated with PLL (Sigma-Aldrich), preformed PLGA nanoparticles (10 mg/ml) in ultrapure water were added dropwise into 1 ml of 0.05% (w/v) PLL under 700 rpm of stirring for 2 hours. Next, five washes were used to remove any free polyelectrolyte, and the PLLNP were resuspended in ultrapure water for further use. To characterize the size and zeta potential of the PLGA cores and PLLNP, the samples were tested using a Zetasizer MAL 1267090 (Malvern Panalytical).

Preparation of RBCNP

RBCNP were prepared by a cell membrane cloaking technique (*50*, *51*). The RBC membrane was mixed with PLGA cores at a 1:1 weight ratio of membrane protein to PLGA polymer. The mixture was then sonicated using a Thermo Fisher Scientific FS30D ultrasonic bath sonicator for 3 min. The RBCNP were isolated by centrifugation for 5 min at 16,100*g* and washed three times with ultrapure water. To characterize the size and surface zeta potential of RBCNP, the samples were tested using a Zetasizer MAL 1267090. To characterize the morphology, the samples were deposited onto a carbon-coated 400-mesh copper grid and stained with 1 wt % of uranyl acetate (Electron Microscopy Sciences), followed by imaging on a JEOL 1200 EX II transmission electron microscope.

Preparation of acido-algae-PLLNP biohybrid motors

To attach PLLNP, 1×10^7 acidophilic algae were first isolated from MAM and resuspended in ultrapure water. Then, the PLLNP were mixed with algae for 30 min. After nanoparticle attachment, the resulting acido-algae-PLLNP biohybrid motors were washed three times and resuspended in ultrapure water.

Preparation of acido-algae-RBCNP biohybrid motors

To conjugate RBCNP onto algae, the acidophilic algae and RBCNP were linked using click chemistry. First, 1×10^7 algae were treated with 20 μM DBCO-PEG_4-NHS (Click Chemistry Tools) for 1 hour at room temperature. The RBCNP were incubated with 20 μM azido-PEG_4-NHS (Click Chemistry Tools) for 1 hour at room

temperature. Both the algae and RBCNP were centrifuged and washed three times with ultrapure water to remove the unreacted NHS esters. Then, the modified algae and RBCNP were mixed and vortexed for 4 hours to complete the click chemistry reaction. After conjugation, the resulting acido-algae-RBCNP biohybrid motors were separated by centrifugation at 800*g* for 3 min, followed by three washes.

Binding stability of acido-algae-PLLNP and acido-algae-RBCNP in acidic conditions

To test the binding stability between PLLNP and acidophilic algae after the formation of biohybrid motors, the acido-algae-PLLNP with DiR loading were incubated with two acidic conditions (simulated gastric fluid and HCl at pH 2) for 24 hours. The detached PLLNP in the supernatant was removed by centrifugation at 800*g* for 3 min. Before and after incubation, the fluorescence intensity of PLLNP with DiR loading on the algae surface was measured using a plate reader. The binding stability of acido-algae-RBCNP was evaluated following the same method.

Motion analysis

The speed of acidophilic algae, neutrophilic algae, fluorescein-conjugated algae motors, acido-algae-PLLNP biohybrid motors, and acido-algae-RBCNP biohybrid motors was analyzed in different media: MAM (pH ~ 3.5), simulated gastric fluid (pH ~ 1.5; RICCA Chemical), simulated intestinal fluid (pH ~ 6.5; RICCA Chemical), 1× PBS (pH ~ 7.4), ultrapure water, pH-adjusted aqueous solutions (pH from 0 to 11), sulfuric acid (pH ~ 1.5; Sigma-Aldrich), and nitric acid (pH ~ 1.5; Thermo Fisher Scientific). The motion of the acidophilic algae motors was also observed in HCl solution (pH ~ 1.5; Sigma-Aldrich) at 0, 1, 4, 8, 24, and 72 hours at room temperature (22°C). Movies were captured by a Nikon Eclipse Ti-S/L100 inverted optical bright-field microscope coupled with 10× or 20× objectives and a Hamamatsu digital camera C11440 or by a Sony RX100 V camera on an Invitrogen EVOS FL fluorescence microscope with 20× or 40× objectives. An NIS Element tracking module was used to measure the speed of the motors in different media. To mimic the conditions in the stomach of mice, simulated gastric fluid containing pepsin (1 mg/ml; Sigma-Aldrich) was used to test the influence of enzymes on the motility of acidophilic algae. Speed was measured after incubation for 0, 1, 2, 4, and 8 hours at body temperature (37°C).

Viability of acidophilic algae motors

To evaluate the viability of acidophilic algae in solutions with different pH, algae were transferred from MAM to aqueous solutions with pH from 0 to 11 and incubated for 2 hours at room temperature (22°C). After incubation, algae motors were resuspended into 5 μM SYTOX green fluorescent probe (Thermo Fisher Scientific) for 1 hour at room temperature (22°C). The viability of the algae was determined by counting the live/dead ratio using an Invitrogen EVOS FL fluorescence microscope.

Characterization of acido-algae-PLLNP and acido-algae-RBCNP biohybrid motors

To visualize nanoparticle binding on the surface of the algae, PLGA cores were loaded beforehand with the fluorescent dye DiO. An Invitrogen EVOS FL microscope was used to capture the autofluorescence of algae chloroplasts in the Cy5 channel and DiO-encapsulated nanoparticles in the GFP channel. To further confirm the morphology of the acido-algae-PLLNP and acido-algae-RBCNP biohybrid motors, SEM imaging was performed. Briefly, the biohybrid motors were fixed with a 2.5% glutaraldehyde solution (Sigma-Aldrich) overnight at 4°C, followed by washing in ultrapure water. The samples were then sputtered with palladium for imaging on a Zeiss Sigma 500 SEM instrument with an accelerating voltage of 3 kV.

Animal care

Mice were housed in an animal facility at the University of California San Diego (UCSD) under federal, state, local, and National Institutes of Health (NIH) guidelines. Mice were maintained in standard housing with cycles of 12-hour light and 12-hour dark, ambient temperature, and normal humidity. All animal experiments were performed in accordance with NIH guidelines and approved by the Institutional Animal Care and Use Committee of UCSD.

Ex vivo GI tract imaging and retention quantification

To study GI tract distribution and retention, 8-week-old male CD-1 mice (Charles River Laboratories) were orally administered with Cy7-conjugated acidophilic algae, Cy7-conjugated static acidophilic algae, or Cy7-conjugated neutrophilic algae in 500 μl of PBS at a concentration of 1×10^7/ml. At the predetermined time points (0.5, 2, 5, 10, and 24 hours), the mice were euthanized, and their GI tracts were excised for analysis. To evaluate the performance of the biohybrid motors in vivo, the mice were orally administered with acido-algae-PLLNP, PLLNP, acido-algae-RBCNP, or RBCNP. At predetermined time points (2, 5, and 10 hours), the mice were euthanized, and their GI tracts were excised for analysis. Fluorescent ex vivo GI images were obtained with the Xenogen IVIS 200 system.

In vivo safety studies

Eight-week-old male CD-1 mice were euthanized at 24 hours after oral administration of algae motors in 500 μl of PBS at a concentration of 1×10^7/ml. For the comprehensive chemistry panel, aliquots of blood were allowed to coagulate, and the serum was collected by centrifugation. To obtain blood cell counts, whole blood was collected into potassium EDTA collection tubes (Sarstedt). Analyses were conducted by the UCSD Animal Care Program Diagnostic Services Laboratory. To perform the histological analysis, different portions of the GI tract and major organs were sectioned and stained with H&E (Leica Biosystems), followed by imaging using a Hamamatsu Nanozoomer 2.0-HT slide scanning system.

Supplementary Materials

This PDF file includes:
Figs. S1 to S17

Other Supplementary Material for this manuscript includes the following:
Movies S1 to S10

REFERENCES AND NOTES

1. G. Z. Yang, J. Bellingham, P. E. Dupont, P. Fischer, L. Floridi, R. Full, N. Jacobstein, V. Kumar, M. McNutt, R. Merrifield, B. J. Nelson, The grand challenges of science robotics. *Sci. Robot.* **3**, eaar7650 (2018).

2. K. L. Smith Jr., A. D. Sherman, P. R. McGill, R. G. Henthorn, J. Ferreira, T. P. Connolly, C. L. Huffard, Abyssal Benthic Rover, an autonomous vehicle for long-term monitoring of deep-ocean processes. *Sci. Robot.* **6**, eabl4925 (2021).
3. H. Singh, T. Maksym, J. Wilkinson, G. Williams, Inexpensive, small AUVs for studying ice-covered polar environments. *Sci. Robot.* **2**, eaan4809 (2017).
4. J. Dupeyroux, J. R. Serres, S. Viollet, AntBot: A six-legged walking robot able to home like desert ants in outdoor environments. *Sci. Robot.* **4**, eaau0307 (2019).
5. A. Ghosh, P. Fischer, Controlled propulsion of artificial magnetic nanostructured propellers. *Nano Lett.* **9**, 2243–2245 (2009).
6. L. Zhang, J. J. Abbott, L. Dong, B. E. Kratochvil, D. Bell, B. J. Nelson, Artificial bacterial flagella: Fabrication and magnetic control. *Appl. Phys. Lett.* **94**, 064107 (2009).
7. B. Dai, J. Wang, Z. Xiong, X. Zhan, W. Dai, C. C. Li, S. P. Feng, J. Tang, Programmable artificial phototactic microswimmer. *Nat. Nanotechnol.* **11**, 1087–1092 (2016).
8. M. Xuan, Z. Wu, J. Shao, L. Dai, T. Si, Q. He, Near infrared light-powered Janus mesoporous silica nanoparticle motors. *J. Am. Chem. Soc.* **138**, 6492–6497 (2016).
9. W. Wang, S. Li, L. Mair, S. Ahmed, T. J. Huang, T. E. Mallouk, Acoustic propulsion of nanorod motors inside living cells. *Angew. Chem. Int. Ed.* **53**, 3201–3204 (2014).
10. A. A. Solovev, Y. Mei, E. Bermúdez Ureña, G. Huang, O. G. Schmidt, Catalytic microtubular jet engines self-propelled by accumulated gas bubbles. *Small* **5**, 1688–1692 (2009).
11. W. F. Paxton, K. C. Kistler, C. C. Olmeda, A. Sen, S. K. St. Angelo, Y. Cao, T. E. Mallouk, P. E. Lammert, V. H. Crespi, Catalytic nanomotors: Autonomous movement of striped nanorods. *J. Am. Chem. Soc.* **126**, 13424–13431 (2004).
12. W. Gao, S. Sattayasamitsathit, J. Orozco, J. Wang, Highly efficient catalytic microengines: Template electrosynthesis of polyaniline/platinum microtubes. *J. Am. Chem. Soc.* **133**, 11862–11864 (2011).
13. X. Ma, A. Jannasch, U. R. Albrecht, K. Hahn, A. Miguel-López, E. Schaffer, S. Sánchez, Enzyme-powered hollow mesoporous Janus nanomotors. *Nano Lett.* **15**, 7043–7050 (2015).
14. W. Gao, A. Pei, J. Wang, Water-driven micromotors. *ACS Nano* **6**, 8432–8438 (2012).
15. J. Wang, *Nanomachines: Fundamentals and Applications* (Wiley-VCH, 2013).
16. M. Medina-Sánchez, L. Schwarz, A. K. Meyer, F. Hebenstreit, O. G. Schmidt, Cellular cargo delivery: Toward assisted fertilization by sperm-carrying micromotors. *Nano Lett.* **16**, 555–561 (2015).
17. D. B. Weibel, P. Garstecki, D. Ryan, W. R. DiLuzio, M. Mayer, J. E. Seto, G. M. Whitesides, Microoxen: Microorganisms to move microscale loads. *Proc. Natl. Acad. Sci. U.S.A.* **102**, 11963–11967 (2005).
18. Y. Alapan, O. Yasa, O. Schauer, J. Giltinan, A. F. Tabak, V. Sourjik, M. Sitti, Soft erythrocyte-based bacterial microswimmers for cargo delivery. *Sci. Robot.* **3**, eaar4423 (2018).
19. O. Felfoul, M. Mohammadi, S. Taherkhani, D. De Lanauze, Y. Z. Xu, D. Loghin, S. Essa, S. Jancik, D. Houle, M. Lafleur, L. Gaboury, M. Tabrizian, N. Kaou, M. Atkin, T. Vuong, G. Batist, N. Beauchemin, D. Radzioch, S. Martel, Magneto-aerotactic bacteria deliver drug-containing nanoliposomes to tumour hypoxic regions. *Nat. Nanotechnol.* **11**, 941–947 (2016).
20. F. Zhang, Z. Li, L. Yin, Q. Zhang, N. Askarinam, R. Mundaca-Uribe, F. Tehrani, E. Karshalev, W. Gao, L. Zhang, J. Wang, ACE2 receptor modified algae-based microrobot for removal of SARS-CoV-2 in wastewater. *J. Am. Chem. Soc.* **43**, 12194–12201 (2021).
21. B. E. F. de Ávila, P. Angsantikul, J. Li, W. Gao, L. Zhang, J. Wang, Micromotors go in vivo: From test tubes to live animals. *Adv. Funct. Mater.* **28**, 1705640 (2018).
22. Y. Alapan, U. Bozuyuk, P. Erkoc, A. C. Karacakol, M. Sitti, Multifunctional surface microrollers for targeted cargo delivery in physiological blood flow. *Sci. Robot.* **5**, eaba5726 (2020).
23. H. Zhang, Z. Li, C. Gao, X. Fan, Y. Pang, T. Li, Z. Wu, H. Xie, Q. He, Dual-responsive biohybrid neutrobots for active target delivery. *Sci Robot.* **6**, eaaz9519 (2021).
24. Z. Wu, J. Troll, H. H. Jeong, Q. Wei, M. Stang, F. Ziemssen, Z. Wang, M. Dong, S. Schnichels, T. Qiu, P. Fischer, A swarm of slippery micropropellers penetrates the vitreous body of the eye. *Sci. Adv.* **4**, eaat4388 (2018).
25. B. Wang, K. F. Chan, K. Yuan, Q. Wang, X. Xia, L. Yang, H. Ko, Y. X. J. Wang, J. J. Y. Sung, P. W. Y. Chiu, L. Zhang, Endoscopy-assisted magnetic navigation of biohybrid soft microrobots with rapid endoluminal delivery and imaging. *Sci. Robot.* **6**, eabd2813 (2021).
26. F. Zhang, J. Zhuang, Z. Li, H. Gong, B. E. F. de Ávila, Y. Duan, Q. Zhang, J. Zhou, L. Yin, E. Karshalev, W. Gao, V. Nizet, R. H. Fang, L. Zhang, J. Wang, Nanoparticle-modified microrobots for in vivo antibiotic delivery to treat acute bacterial pneumonia. *Nat. Mater.* **21**, 1324–1332 (2022).
27. R. Mundaca-Uribe, E. Karshalev, B. E. F. de Ávila, X. Wei, B. Nguyen, I. Litvan, R. H. Fang, L. Zhang, J. Wang, A microstirring pill enhances bioavailability of orally administered drugs. *Adv. Sci.* **8**, 2100389 (2021).
28. F. Zhang, Z. Li, Y. Duan, A. Abbas, R. Mundaca-Uribe, L. Yin, H. Luan, W. Gao, R. H. Fang, L. Zhang, J. Wang, Gastrointestinal tract drug delivery using algae motors embedded in a degradable capsule. *Sci. Robot.* **7**, eabo4160 (2022).
29. J. N. Chu, G. Traverso, Foundations of gastrointestinal-based drug delivery and future developments. *Nat. Rev. Gastroenterol. Hepatol.* **19**, 219–238 (2022).
30. A. M. Bellinger, M. Jafari, T. M. Grant, S. Zhang, H. C. Slater, E. A. Wenger, S. Mo, Y. A. L. Lee, H. Mazdiyasni, L. Kogan, R. Barman, C. Cleveland, L. Booth, T. Bensel, D. Minahan, H. M. Hurowitz, T. Tai, J. Daily, B. Nikolic, L. Wood, P. A. Eckhoff, R. Langer, G. Traverso, Oral, ultra–long-lasting drug delivery: Application toward malaria elimination goals. *Sci. Transl. Med.* **8**, 365ra157 (2016).
31. A. Abramson, E. Caffarel-Salvador, M. Khang, D. Dellal, D. Silverstein, Y. Gao, M. R. Frederiksen, A. Vegge, F. Hubálek, J. J. Water, A. V. Friderichsen, J. Fels, R. K. Kirk, C. Cleveland, J. Collins, S. Tamang, A. Hayward, T. Landh, S. T. Buckley, N. Roxhed, U. Rahbek, R. Langer, G. Traverso, An ingestible self-orienting system for oral delivery of macromolecules. *Science* **363**, 611–615 (2019).
32. A. Abramson, M. R. Frederiksen, A. Vegge, B. Jensen, M. Poulsen, B. Mouridsen, M. O. Jespersen, R. K. Kirk, J. Windum, F. Hubálek, J. J. Water, J. Fels, S. B. Gunnarsson, A. Bohr, E. M. Straarup, M. W. H. Ley, X. Lu, J. Wainer, J. Collins, S. Tamang, K. Ishida, A. Hayward, P. Herskind, S. T. Buckley, N. Roxhed, R. Langer, U. Rahbek, G. Traverso, Oral delivery of systemic monoclonal antibodies, peptides and small molecules using gastric auto-injectors. *Nat. Biotechnol.* **40**, 103–109 (2022).
33. D. Walker, B. T. Käsdorf, H.-H. Jeong, O. Lieleg, P. Fischer, Enzymatically active biomimetic micropropellers for the penetration of mucin gels. *Sci. Adv.* **1**, e1500501 (2015).
34. W. Gao, M. D'Agostino, V. Garcia-Gradilla, J. Orozco, J. Wang, Multi-fuel driven janus micromotors. *Small* **9**, 467–471 (2013).
35. B. E. F. de Ávila, P. Angsantikul, J. Li, M. A. Lopez-Ramirez, D. E. Ramírez-Herrera, S. Thamphiwatana, C. Chen, J. Delezuk, R. Samakapiruk, V. Ramez, M. Obonyo, L. Zhang, J. Wang, Micromotor-enabled active drug delivery for in vivo treatment of stomach infection. *Nat. Commun.* **8**, 272 (2017).
36. W. Gao, R. Dong, S. Thamphiwatana, J. Li, W. Gao, L. Zhang, J. Wang, Artificial micromotors in the mouse's stomach: A step toward in vivo use of synthetic motors. *ACS Nano* **9**, 117–123 (2015).
37. N. Merino, H. S. Aronson, D. P. Bojanova, J. Feyhl-Buska, M. L. Wong, S. Zhang, D. Giovannelli, Living at the extremes: Extremophiles and the limits of life in a planetary context. *Front. Microbiol.* **10**, 780 (2019).
38. S. Hirooka, Y. Hirose, Y. Kanesaki, S. Higuchi, T. Fujiwara, R. Onuma, A. Era, R. Ohbayashi, A. Uzuka, H. Nozaki, H. Yoshikawa, Acidophilic green algal genome provides insights into adaptation to an acidic environment. *Proc. Natl. Acad. Sci. U.S.A.* **114**, E8304–E8313 (2017).
39. D. B. Johnson, Acidophilic algae isolated from mine-impacted environments and their roles in sustaining heterotrophic acidophiles. *Front. Microbiol.* **3**, 325 (2012).
40. W. Gross, Ecophysiology of algae living in highly acidic environments. *Hydrobiologia* **433**, 31–37 (2000).
41. A. P. Dean, A. Hartley, O. A. McIntosh, A. Smith, H. K. Feord, N. H. Holmberg, T. King, E. Yardley, K. N. White, J. K. Pittman, Metabolic adaptation of a Chlamydomonas acidophila strain isolated from acid mine drainage ponds with low eukaryotic diversity. *Sci. Total Environ.* **647**, 75–87 (2019).
42. M. M. Olaueson, P. M. Stokes, Responses of the acidophilic alga Euglena Mutabilis (Euglenophyceae) to carbon enrichment at pH 3. *J. Phycol.* **25**, 529–539 (1989).
43. O. Yasa, P. Erkoc, Y. Alapan, M. Sitti, Microalga-powered microswimmers toward active cargo delivery. *Adv. Mater.* **30**, 1804130 (2018).
44. L. M. Ensign, R. Cone, J. Hanes, Oral drug delivery with polymeric nanoparticles: The gastrointestinal mucus barriers. *Adv. Drug Deliv. Rev.* **64**, 557–570 (2012).
45. A. Brodkorb, L. Egger, M. Alminger, P. Alvito, R. Assunção, S. Ballance, T. Bohn, C. Bourlieu-Lacanal, R. Boutrou, F. Carrière, A. Clemente, M. Corredig, D. Dupont, C. Dufour, C. Edwards, M. Golding, S. Karakaya, B. Kirkhus, S. Le Feunteun, U. Lesmes, A. Macierzanka, A. R. Mackie, C. Martins, S. Marze, D. J. McClements, O. Ménard, M. Minekus, R. Portmann, C. N. Santos, I. Souchon, R. P. Singh, G. E. Vegarud, M. S. J. Wickham, W. Weitschies, I. Recio, INFOGEST static in vitro simulation of gastrointestinal food digestion. *Nat. Protoc.* **14**, 991–1014 (2019).
46. M. Y. Inoue, K. Izawa, S. Kiryu, A. Tojo, K. Ohtomo, Diet and abdominal autofluorescence detected by in vivo fluorescence imaging of living mice. *Mol. Imaging* **7**, 7290 (2008).
47. M. N. Kamaly, Z. Xiao, P. M. Valencia, A. F. Radovic-Moreno, O. C. Farokhzad, Targeted polymeric therapeutic nanoparticles: Design, development and clinical translation. *Chem. Soc. Rev.* **41**, 2971–3010 (2012).
48. M. S. Honary, F. Zahir, Effect of zeta potential on the properties of nano-drug delivery systems—A review (part 1). *Trop. J. Pharm. Res.* **12**, 255–264 (2013).
49. X. Wei, M. Beltrán-Gastélum, E. Karshalev, B. E.-F. de Ávila, J. Zhou, D. Ran, P. Angsantikul, R. H. Fang, J. Wang, L. Zhang, Biomimetic micromotor enables active delivery of antigens for oral vaccination. *Nano Lett.* **19**, 1914–1921 (2019).
50. R. H. Fang, A. V. Kroll, W. Gao, L. Zhang, Cell membrane coating nanotechnology. *Adv. Mater.* **30**, e1706759 (2018).
51. J. A. Copp, R. H. Fang, B. T. Luk, C. M. J. Hu, W. Gao, K. Zhang, L. Zhang, Clearance of pathological antibodies using biomimetic nanoparticles. *Proc. Natl. Acad. Sci. U.S.A.* **111**, 13481–13486 (2014).

52. Q. Hu, W. Sun, J. Wang, H. Ruan, X. Zhang, Y. Ye, S. Shen, C. Wang, W. Lu, K. Cheng, G. Dotti, J. F. Zeidner, J. Wang, Z. Gu, Conjugation of haematopoietic stem cells and platelets decorated with anti-PD-1 antibodies augments anti-leukaemia efficacy. *Nat. Biomed. Eng.* **2**, 831–840 (2018).
53. S. Hellmig, F. Von Schöning, C. Gadow, S. Katsoulis, J. Hedderich, U. R. Fölsch, E. Stüber, Gastric emptying time of fluids and solids in healthy subjects determined by 13C breath tests: Influence of age, sex and body mass index. *J. Gastroenterol. Hepatol.* **21**, 1832–1838 (2016).
54. H. K. Makadia, S. J. Siegel, Poly lactic-co-glycolic acid (PLGA) as biodegradable controlled drug delivery carrier. *Polymers* **3**, 1377–1397 (2011).
55. J. M. Hyman, E. I. Geihe, B. M. Trantow, B. Parvin, P. A. Wender, A molecular method for the delivery of small molecules and proteins across the cell wall of algae using molecular transporters. *Proc. Natl. Acad. Sci. U.S.A.* **109**, 13225–13230 (2012).
56. C. Lautenschläger, C. Schmidt, D. Fischer, A. Stallmach, Drug delivery strategies in the therapy of inflammatory bowel disease. *Adv. Drug Deliv. Rev.* **71**, 58–76 (2014).

Acknowledgments
Funding: This work is supported by the Defense Threat Reduction Agency Joint Science and Technology Office for Chemical and Biological Defense under grant number HDTRA1-21-1-0010 and the National Science Foundation grant DMR-1904702. **Author contributions:** F.Z., Z.L., L.Z., and J.W. conceived the ideas. F.Z., Z.L., and Y.D. designed the in vitro, in vivo, and ex vivo experiments. F.Z., Z.L., H.L., and Z.G. conducted in vitro fabrication and characterization of the algae-based motor formulation. Z.L., H.L., and M.X. performed speed measurements. Y.D. and F.Z. performed the in vivo and ex vivo experiments. F.Z., Z.L., Y.D., L.Y., and C.C. prepared the figures. F.Z., R.H.F., L.Z., and J.W. wrote the manuscript with inputs from all authors. L.Z. and J.W supervised the project. All the authors contributed to the discussion and analysis of the data. **Competing interests:** The authors declare that they have no competing interests. **Data and materials availability:** All data needed to evaluate the conclusions in the paper are present in the paper and/or the Supplementary Materials.

Submitted 30 August 2022
Accepted 7 November 2022
Published 23 December 2022
10.1126/sciadv.ade6455